Estuaries and Coasts
https://doi.org/10.1007/s12237-019-00564-8

SPECIAL ISSUE: IMPACT OF 2017 HURRICANES

Mangrove Damage, Delayed Mortality, and Early Recovery Following Hurricane Irma at Two Landfall Sites in Southwest Florida, USA

Kara R. Radabaugh[1] · Ryan P. Moyer[1] · Amanda R. Chappel[1] · Emma E. Dontis[1] · Christine E. Russo[1] · Kristen M. Joyse[2] · Melissa W. Bownik[3] · Audrey H. Goeckner[3,4] · Nicole S. Khan[5]

Received: 14 January 2019 / Revised: 3 April 2019 / Accepted: 9 April 2019

Abstract

Mangrove forests along the coastlines of the tropical and sub-tropical western Atlantic are intermittently impacted by hurricanes and can be damaged by high-speed winds, high-energy storm surges, and storm surge sediment deposits that suffocate tree roots. This study quantified trends in damage, delayed mortality, and early signs of below- and aboveground recovery in mangrove forests in the Lower Florida Keys and Ten Thousand Islands following direct hits by Hurricane Irma in September 2017. Mangrove trees suffered 19% mortality at sites in the Lower Florida Keys and 11% in the Ten Thousand Islands 2–3 months post-storm; 9 months post-storm, mortality in these locations increased to 36% and 20%, respectively. Delayed mortality of mangrove trees was associated with the presence of a carbonate mud storm surge deposit on the forest floor. Mortality and severe branch damage were more common for mangrove trees than for mangrove saplings. Canopy coverage increased from 40% cover 1–2 months post-storm to 60% cover 3–6 months post-storm. Canopy coverage remained the same 9 months post-storm, providing light to an understory of predominantly *Rhizophora mangle* (red mangrove) seedlings. Soil shear strength was higher in the Lower Florida Keys and varied with depth; no significant trends were found in shear strength between fringe or basin plots. Rates of root growth, as assessed using root in-growth bags, were relatively low at 0.01–11.0 g m^{-2} $month^{-1}$ and were higher in the Ten Thousand Islands. This study demonstrated that significant delayed mangrove mortality can occur 3–9 months after a hurricane has passed, with some mortality attributable to smothering by storm surge deposits.

Keywords Hurricane · Mangrove · Storm deposit · Shear strength · Root growth

Introduction

Mangrove forests grow along coastal zones with temperate to tropical climates, and many of these areas are subject to periodic damage caused by tropical cyclone winds and storm surges (Sippo et al. 2018; Simard et al. 2019). These severe ecosystem disturbances can defoliate the canopy, snap branches and trunks, damage bark, and uproot trees, resulting in the destruction of the predominant canopy in a mangrove forest (Everham and Brokaw 1996; Zhang et al. 2008; Smith III et al. 2009; Villamayor et al. 2016; Han et al. 2018). The extent of major damage to the canopy, but not necessarily total mortality, is largely dependent on wind speed, gustiness, and wind direction (Everham and Brokaw 1996; Han et al. 2018; Imbert 2018). The degree of damage during a tropical cyclone and subsequent recovery of mangrove forests vary widely by species (Roth 1992; Baldwin et al. 1995, 2001; Imbert et al. 1996; McCoy et al. 1996; Feller et al. 2015; Villamayor et al. 2016; Imbert 2018), hydrogeomorphic forest type (Craighead

Communicated by Dan Friess

✉ Kara R. Radabaugh
kara.radabaugh@myfwc.com

[1] Florida Fish and Wildlife Conservation Commission, Fish and Wildlife Research Institute, 100 Eighth Avenue Southeast, Saint Petersburg, FL 33701, USA

[2] Department of Earth and Planetary Sciences, Rutgers University, 610 Taylor Road, Piscataway, NJ 08854, USA

[3] University of South Florida, 4202 East Fowler Ave, Tampa, FL 33620, USA

[4] Gulf Coast Research and Education Center, University of Florida, 14625 County Road 672, Wimauma, FL 33598, USA

[5] Asian School of the Environment, Nanyang Technological University, 50 Nanyang Avenue, N1.3 B1-15, Singapore 639798, Singapore

Published online: 29 April 2019

and Gilbert 1962; Cahoon et al. 2003; Smith III et al. 2009; Han et al. 2018; Imbert 2018), forest age structure (Smith III et al. 1994; Sherman et al. 2001; Villamayor et al. 2016), and thickness of deposits left by the storm surge (Craighead and Gilbert 1962; Risi et al. 1995; Ellison 1998).

Mangroves exhibit species-specific responses to the damage caused by tropical cyclones. Species in the genera *Avicennia* and *Laguncularia* grow epicormic sprouts in response to canopy damage and therefore tend to have lower mortality following storm damage (Tomlinson 1980; Baldwin et al. 1995, 2001; Imbert et al. 1996; McCoy et al. 1996; Imbert 2018). Species belonging to the genus *Rhizophora* do not exhibit epicormic growth following tropical cyclone damage because they lack viable dormant buds in mature trunks and branches and are thus highly susceptible to mortality post-cyclone (Tomlinson 1980; Baldwin et al. 1995, 2001; Imbert et al. 1996; Villamayor et al. 2016; Imbert 2018). However, *Rhizophora mangle* (red mangrove) seedlings in Florida and the Caribbean are often present in relatively high densities in the forest understory and therefore poised for rapid growth when gaps are created by canopy disturbance (Walker et al. 1991; Everham and Brokaw 1996; Baldwin et al. 2001; Ross et al. 2006; Imbert 2018).

Storm surges have varying impacts on mangrove forests. Powerful wave energy can erode the shoreline or uproot trees, yet submergence by storm surge can protect smaller saplings against defoliation by high-speed winds (Smith III et al. 1994). Allochthonous sediment, composed of a mixture of grain sizes (sand–mud) and mineral compositions (carbonate and siliciclastic), is carried in by storm surges and deposited on the forest floor as the water recedes (Risi et al. 1995). These storm deposits are important contributors of nutrient resources and substrate elevation in mangrove forests (Castañeda-Moya et al. 2010), which can help forests keep pace with sea-level rise (Krauss et al. 2014; Breithaupt et al. 2017). However, thick storm deposits can also be detrimental to the mangrove trees themselves as these sediments can interfere with the gas exchange of roots and soil, smother roots, and result in delayed tree mortality (Craighead and Gilbert 1962; Ellison 1998). Silt and clay deposits result in higher mortality compared with sand, presumably because soil aeration declines with decreasing grain size (Ellison 1998). Stagnant water, which may occur following a tropical cyclone due to altered hydrology, can similarly interfere with gas exchange, smother roots, and cause delayed mortality (Allingham and Neil 1996; Lewis III et al. 2016). Thus, initial estimates of tree mortality often underestimate the full impact of a storm event because mangrove trees that initially survive the storm may later die from lack of oxygen uptake by their roots (Craighead and Gilbert 1962).

Forests can follow four recovery trajectories following a severe wind event: regrowth (surviving trees begin to grow again), recruitment (new growth of early successional species), release (rapid growth of the existing understory), or repression (invasion of herbaceous plants) (Everham and Brokaw 1996). With the exception of possible adjacent salt marshes, mangrove forests generally lack herbaceous plants or early successional species; thus, they primarily recover following the trajectories of regrowth or release. Florida and Caribbean mangrove forests have low species diversity and are dominated by only three mangrove species: *R. mangle*, *Avicennia germinans* (black mangrove), and *Laguncularia racemosa* (white mangrove); however, recovery into a comparable mangrove forest is not guaranteed (Craighead 1971; Smith III et al. 1994; Imbert et al. 1996; Baldwin et al. 2001). Species composition of recovering mangrove forests may therefore largely depend upon the "released" growth of the understory, including small, yet established, saplings growing in canopy gaps prior to the tropical cyclone (Smith III et al. 1994) as well as seedlings that survive the storm (Baldwin et al. 2001).

The objective of this study was to quantify trends in damage, delayed mortality, and below- and aboveground signs of recovery of mangrove forests following direct hits by Hurricane Irma in the Lower Florida Keys and Ten Thousand Islands. While numerous studies have examined mangrove forest damage and recovery following tropical cyclones, this study adds to a small body of literature quantifying the degree of delayed mortality that can occur in the months following a major storm (Smith III et al. 1994; Sherman et al. 2001; Barr et al. 2012), particularly when associated with storm surge deposits (Craighead and Gilbert 1962; Ellison 1998; Smith III et al. 2009).

Methods

Study Sites

Study sites in the Lower Florida Keys (Fig. 1a) were located on uninhabited mangrove islands within the Great White Heron National Wildlife Refuge. The substrate on these mangrove islands included a layer of mangrove peat mixed with calcareous mud on a bedrock of Miami limestone (Ross et al. 1992). The fringes of the mangrove forests were dominated by *R. mangle*, with scattered *A. germinans* and *L. racemosa* intermixed with *R. mangle* in the forest basins. Study sites were tall mangrove forests with the exception of the forest basins at Upper Saddlebunch Key and Mud Key, which contained smaller scrub mangroves.

Located on the coast of Collier County, the Ten Thousand Islands region is largely undeveloped with the exception of Marco Island (Fig. 1b). The coast is protected by an assortment of public lands, including the Rookery Bay Aquatic

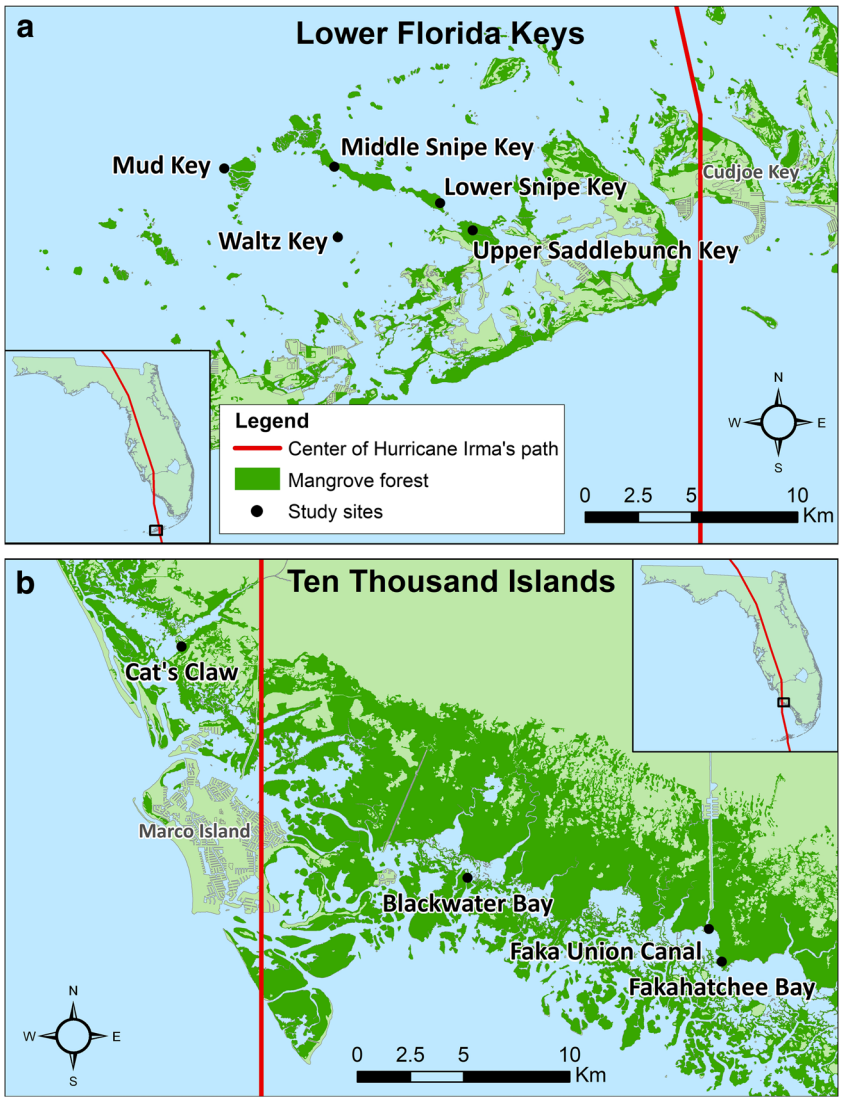

Fig. 1 Study sites, mangrove extent (FNAI and FWC 2016), and path of Hurricane Irma (NOAA 2017) as it made landfall as a category 4 hurricane in the Lower Florida Keys (**a**) and a category 3 hurricane in the Ten Thousand Islands (**b**) in the state of Florida, USA (inset panels). The nine study sites included 18 fringe or basin plots (see Table 1)

Preserve, Rookery Bay National Estuarine Research Reserve, Cape Romano-Ten Thousand Islands Aquatic Preserve, Ten Thousand Islands National Wildlife Refuge, and Everglades National Park. The many coastal islands which give the Ten Thousand Islands its name originated as reefs of oysters and vermetid gastropods, which were later colonized by mangroves (Shier 1969). The substrate of mangrove forests located in southwest Florida consists of a layer of mangrove peat on top of shell hash, quartz sand, and limestone. Species composition at the Ten Thousand Islands sites was similar to that of the Lower Florida Keys, with *R. mangle* dominating the fringe, and *A. germinans* and *L. racemosa* intermixed with *R. mangle* in forest basins.

Both the Florida Keys and southwest Florida frequently experience powerful tropical cyclones (referred to as "hurricanes" in the western North Atlantic and subbasins). Major historical hurricanes include the 1935 Labor Day hurricane, a category 5 on the Saffir–Simpson hurricane wind scale that crossed the Lower Florida Keys and traveled up the west coast of Florida. Hurricane Donna also crossed the Keys as a category 4 hurricane in 1960 and made landfall on southwest Florida (Craighead and Gilbert 1962; NOAA 2019). Hurricane Andrew made landfall in 1992 in southeast Florida as a category 5 hurricane and crossed over to southwest Florida as a category 4 (NOAA 2019). Hurricane Wilma made landfall in 2005 near Marco Island and the Ten Thousand Islands as a category 3 hurricane (NOAA 2019). Many of the mangrove forests in south Florida are second-growth forests as a result of the loss of large, mature mangroves due to these repetitive hurricanes (Craighead and Gilbert 1962; Smith III et al. 1994; McCoy et al. 1996; Zhang et al. 2008; Han et al. 2018; Sippo et al. 2018).

Hurricane Irma

Hurricane Irma originated on the west coast of Africa on 27 August 2017. It grew into a category 5 hurricane as it crossed the Atlantic Ocean and, at its most intense, had a maximum wind speed of 287 km h^{-1} (Cangialosi et al. 2018). Irma intermittently weakened as it passed over the Caribbean islands and was particularly weakened by Cuba, but it strengthened back into a category 4 storm over the warm waters of the Florida Straits (Cangialosi et al. 2018; Wachnicka et al., in review). Irma made landfall at Cudjoe Key in the Lower Florida Keys (Fig. 1a) on the morning of 10 September 2017 with maximum winds of 213 km h^{-1}. Combined storm surge and tide resulted in maximum inundation levels of 1.5–2.4 m for the Lower Florida Keys. The highest recorded high-water mark was surveyed at 1.66 m above ground level (2.05 m NAVD88/2.07 m mean higher high water (MHHW); Cangialosi et al. 2018).

Within five hours, Irma weakened to a category 3 hurricane and made landfall in southwest Florida near Marco Island in the afternoon of the same day (Fig. 1b). Maximum wind speeds were 185 km h^{-1} (Cangialosi et al. 2018). Strong offshore winds initially blew water away from the shore and caused water levels to drop to 1.46 m below MHHW. Following landfall, inundation in southwest Florida was 1.8–3.0 m above ground level within Everglades National Park and the Ten Thousand Islands National Wildlife Refuge. A storm tide sensor in Everglades City recorded a water level of 2.53 m (NAVD88/2.29 m MHHW). Irma moved north-northwest across southwest Florida but weakened quickly to a category 2 hurricane as it passed by Naples and Fort Myers and became a category 1 hurricane as the center of the storm passed between Tampa and Orlando. The hurricane brought heavy rainfall, with 25–38 cm precipitation recorded in the Keys and peninsular Florida (Cangialosi et al. 2018).

The eye of Hurricane Irma was 28–37 km in diameter hours prior to landfall in the Florida Keys (NWS 2017a, b). The center of Hurricane Irma's path was within 20.5 km of the Lower Florida Keys sites in this study and within 19.3 km of the Ten Thousand Islands sites. Most Lower Florida Keys sites, with the exception of Mud Key, were within the eyewall of Hurricane Irma and were likely subjected to maximum wind speeds from the hurricane (Willoughby and Rahn 2004; Zhang et al. 2008). The exact eyewall diameter prior to making landfall in the Ten Thousand Islands was not similarly reported, but given the tendency for larger eyewall diameters in storms of decreasing intensity (Willoughby and Rahn 2004; Zhang et al. 2008), it is likely that all sites in the Ten Thousand Islands also experienced the maximum wind speeds of the eyewall.

Sampling Design

A total of 18 permanent monitoring plots (10 × 10 m) were created following the hurricane to monitor above- and below-ground indicators of mangrove mortality and early recovery. Plots were placed adjacent to previously established stratigraphy transects in both fringe and basin mangrove forests. This previous stratigraphy study did not focus on vegetation characteristics; therefore, pre-storm data are not available for comparison. Fringe plots were placed approximately 15 m from the water's edge and basin plots were located 50–100 m from the water's edge adjacent to the transect in the basin forest.

Eleven monitoring plots were established on five islands in the Lower Florida Keys. These included one basin and one fringe plot at Lower Snipe Key, Mud Key, and Upper Saddlebunch Key (Fig. 1a). Two fringe plots were established on Waltz Key (no basin plot due to the lack of a basin forest on the narrow island). Three plots were established on Middle Snipe Key (two fringe and one basin) due to widely variable hurricane damage on either side of the island. Lower Florida Keys vegetation monitoring was conducted in November 2017, March 2018, and June 2018 (2, 6, and 9 months post-storm).

Seven monitoring plots were established at four study sites in the Ten Thousand Islands (Fig. 1b). One basin and one fringe plot were established at Fakahatchee Bay and the Faka Union Canal. Blackwater Bay included a fringe plot on a small overwash island and a basin plot on a nearby larger island. Cat's Claw Basin included only a basin plot, as there was no fringe forest due to a pre-existing overwash berm. Ten Thousand Islands vegetation monitoring was conducted in October 2017 (tree height and canopy measurements only), December 2017, January 2018, and June 2018 (1, 3, 4, and 9 months post-storm).

Field Monitoring

The 10 × 10-m monitoring plots were outlined with a transect tape; trees at the four corners of the plot were flagged to enable plot identification during follow-up monitoring. Canopy cover was determined using a convex spherical densiometer (Forest Densiometers, Rapid City, SD) at the four corners of the plot. Tree height was calculated for ten canopy trees or saplings within or near the plot using a tape measure and clinometer (Suunto, Vantaa, Finland).

Mangroves were classified as trees if the stem diameter at 130 cm above the ground (D_{130}) exceeded 5 cm. Remaining mangroves were classified as saplings ($D_{130} < 5$ cm and height ≥ 1 m) or seedlings (height < 1 m). Mangrove species, D_{130}, and status were recorded for all trees in the 10 × 10-m plots. Status included the condition (live, recently dead, or decayed) and state of the trunk and branches using categories derived from Baldwin et al. (1995). Trees, saplings, and

seedlings were classified as "live" if they had any green foliage (including epicormic growth); dead mangroves had no live foliage. Trunk damage categories included: snap (trunk broken above ground level), tip-up (roots pulled up), lean (< 45° from vertical, natural growth patterns excluded), severe lean (> 45° from vertical, natural growth patterns excluded), or no impact (Baldwin et al. 1995). Branch damage was classified as low, moderate, or severe. If trees had multiple trunks that diverged below 130 cm, each trunk was treated as an individual tree and separate measurements were made. Trees were measured during November/December 2017 and June 2018 monitoring.

Within each 10 × 10-m plot, a nested 5 × 5-m subplot was created in the corner that was most representative of the plot as a whole for sapling and seedling distribution. The same subplot was monitored in each follow-up survey. For all saplings within the 5 × 5-m subplot, the species, condition, trunk status, and branch status were determined following the same categories as trees. The total numbers of live and dead mangrove seedlings were recorded, as well as approximate percent species composition. The tree, sapling, and seedling surveys that were conducted during the initial monitoring (2–3 months post-storm) are assumed to account for all mangroves that were present prior to the storm.

Percent cover of downed wood was estimated using a point-transect method. A 10-m transect was extended in five random compass headings from the center of the 10 × 10-m plot. The type of substrate or organic material (including recent or decayed wood debris) was recorded every meter, resulting in a survey of 50 points within and around the plot.

A shear vane kit was used to determine soil shear strength (the amount of torque required to shear or break apart soil; Poulos 1981). A 5-cm shear vane attached to a direct-reading torque gauge (H-4227, Humboldt Manufacturing, Elgin, IL) was used to measure soil strength in five haphazard locations within the 10 × 10-m plot. At each location, soil strength was measured at the surface and at depths of 25 cm and 50 cm. Measurements were taken by inserting the shear vane into the soil to the desired depth, twisting the vane until soil failure, and reading the torque gauge. Calibration for the friction of the rod without the shear vane was conducted once per site for the 25- and 50-cm depths.

Carbonate mud thickness was measured during each monitoring visit by removing a sediment sample with a thin gouge auger or knife in 2–3 locations, either along the adjacent stratigraphy transect or directly outside the vegetation plots. The carbonate mud thickness exhibited wide variability both within plots and among sites; in addition, mud thicknesses were observed to change in the same location on repeated visits. However, the range of the mud thicknesses at each of the plots could consistently be generalized into three arbitrary categories: minimal to none (no visible deposit or only a veneer < 2 mm in thickness), moderate (0.2–1-cm deposit), or thick (1–9-cm deposit).

To estimate belowground root production, pairs of root ingrowth bags were installed adjacent to permanent monitoring plots. Cylindrical root bags (30 cm height × 5 cm diameter) were constructed from nylon mesh (with expandable 3-mm^2 apertures) sewn with nylon upholstery thread. Root bags were filled with sphagnum peat moss (Lambert Canadian peat moss, Québec, Canada) that had been passed through a 5-mm sieve. The use of root-free soil allows for any root growth within the root bag to be considered new production (Symbula and Day Jr. 1988; Sánchez 2005). To deploy root bags, a "Russian-type" half cylinder peat corer (Eijkelkamp USA, Morrisville, NC) was used to remove a volume of sediment that matched root bag dimensions. Bags were inserted in the hole and held in place with surveyor flags. After retrieval, it was determined that root bags were compressed to an average length of 24 cm when they were inserted into the ground. Root bags were deployed in November 2017 and retrieved in March 2018 at the Lower Florida Keys sites (4-month incubation time); bags were deployed in December 2017 and retrieved in June 2018 at the Ten Thousand Island sites (6-month incubation). Bags were extracted by carefully cutting a wide-diameter circle around the root bag with a hand saw. The root bag was then removed from the ground using a shovel with surrounding soil intact, then carefully separated from the soil using scissors to trim penetrating roots. Root bags were refrigerated upon return to the lab until analyzed.

Laboratory Analysis of Root Bags

Root material and peat were trimmed from the outside of the root bags. Peat was removed from the root bag in subsections, and roots were extracted from the soil with forceps and placed in water to rinse them free of soil and test for flotation (McKee 2001). New root growth was identified by their light color, smooth texture, turgid or elastic structure, or ability to float (Symbula and Day Jr. 1988; McKee 2001; Sánchez 2005). Once all visible roots were removed, the remaining peat was placed in a 2-mm sieve and rinsed to identify additional roots. Floating roots were removed from the sieve catch pan. Cleaned roots were placed in a pre-weighed petri dish and examined under a microscope to verify all roots were new growth rather than peat moss material. Roots were placed in the drying oven at 60 °C until they no longer lost water weight (1–5 days), then weighed to determine dry mass.

Data Analysis

Statistical analyses were conducted using Version 7.15 of the SAS System for Windows (Copyright © 2017, SAS Institute Inc., Cary, NC, USA); a p value less than or equal to an alpha of 0.05 was considered significant. Data were examined for normality using a combination of Shapiro–Wilk tests, probability plots, and quantile plots. Non-normal datasets were

transformed or assessed with non-parametric analyses. A two-tailed *t* test was used to compare tree height across the two regions. Linear regression analyses were used to examine the relationship between woody debris and tree height. Pearson's Chi-Square tests were used to assess branch damage and mortality distributions between trees vs. saplings and among trees in various diameter categories. The Likelihood Ratio Chi-Square test was used instead of the Pearson's Chi-Square if over 50% of the categorical cells had frequency counts less than five.

Multilevel-mixed models with type II hypotheses were used to analyze the impacts of the region, forest type (fringe vs. basin), and storm deposit category on initial tree mortality and delayed tree mortality. The proportion of trees killed was transformed via an arcsine transformation; changes in mortality data over time were not transformed. Basal area, tree height, the proportion of trees with severe branch damage (arcsine transformed), and seedling density were compared across the sediment deposition categories using Fisher's classic one-way ANOVA. A Kruskal-Wallis test was used to assess delayed mortality in saplings across storm deposit categories. Multilevel-mixed models with type II hypotheses were used to analyze the impacts of the region, forest type, monitoring round, soil depth, and/or storm deposit category on soil shear strength and root growth rates, which were both log-transformed ($\log_{10}$). Pearson's correlation coefficient was used to assess the relationship between root growth rate and mangrove height as well as percent species composition (arcsine transformed). Regional data parameters are generally depicted separately if there were significant regional differences and together if there were no significant differences.

Results

Damage was extensive in the monitored mangrove sites in both the Lower Florida Keys and the Ten Thousand Islands (Fig. 2, Table 1), although the severity of damage and depths of storm deposits varied greatly among islands as well as across plots on the same island. In the Lower Florida Keys, 12% of trees snapped, while 4% exhibited a lean or tip-up 2 months post-storm. Tree impacts were similar in the Ten Thousand Islands (14% snapped, 3% lean or tip-up). Many of the trees that initially survived, including some with extensive epicormic growth, died in the months following the hurricane. Unless otherwise noted, all mortality metrics refer to recent mortality (presumably due to the hurricane or its aftereffects) and exclude decaying trees. Two months after Hurricane Irma, average tree mortality in the Lower Florida Keys was 18.6% (range 0–75% mortality across plots); 9 months post-storm, tree mortality increased to 36.6% (13–100% range; Table 1). Three months following the storm, average tree mortality in the Ten Thousand Islands was 11.2% (0–35% range); 9 months post-storm, tree mortality increased to 19.8% (6–35% range; Table 1). This equates to a loss of 40.8% of basal area in the Lower Florida Keys and 17.5% in the Ten Thousand Islands 9 months after the storm. There were no significant differences in initial tree mortality between the two regions, nor between the fringe and basin sites (Table 2). A total of 493 trees were measured 2–3 months post-storm, and 416 trees were measured 9 months post-storm. Variability in tree number was due to loss of trees (only standing trees measured), growth of saplings, and sampling variability when extending transect tapes to outline plots during repeated monitoring efforts.

Extensive epicormic growth was noted on *A. germinans* and *L. racemosa* trees across both regions (Fig. 2). Canopy coverage was near 40% 1–2 months after the storm, then increased and plateaued at approximately 60% 3–6 months post-storm (Fig. 3). Mangroves were significantly taller at sites in the Ten Thousand Islands than the Lower Florida Keys (t_2 test value = 3.18, $p = 0.006$, df = 16). Average tree height ranged from 1.5–8.5 m at sites in the Lower Florida Keys and 5.4–10.6 m at sites in the Ten Thousand Islands (Table 1). Percent cover of new woody debris on the forest floor had a significant positive relationship with tree height (Fig. 4); this relationship was not significant for decayed woody debris (linear regression $R^2 = 0.129$, slope $p = 0.144$, $n = 18$).

Forests were dominated by *R. mangle* and by trees with a D_{130} less than 10 cm (Fig. 5a). While most sites were dominated by trees, two basin sites (Upper Saddlebunch Key and Mud Key) were dominated by scrub mangroves ≤ 2.2 m in height. The proportion of severe branch damage among standing trees was not evenly distributed among size classes, and trees with a $D_{130} \leq 10$ cm had less branch damage than would be expected by chance (Fig. 5b; Likelihood Ratio χ^2 (10, n = 327) = 36.3, $p < 0.0001$). Initial mortality (2–3 months post-storm) was evenly distributed among the size classes (Fig. 5c; Likelihood Ratio χ^2 (5, $n = 327$) = 0.986, $p = 0.964$). Mortality continued to increase several months following the storm (Fig. 5c). Although smaller tree classes (5–10 cm) had lower mortality, the mortality distribution was not significantly different among size classes in June 2018, 9 months post-storm (Fig. 5c; Likelihood Ratio χ^2 (5, $n = 309$) = 5.710, p = 0.336). In the initial monitoring surveys 2–3 months post-storm, mortality was significantly higher for trees compared with saplings (Pearson's χ^2 (1, $n = 673$) = 9.33, $p = 0.002$). Severe branch damage was also significantly higher for trees (Pearson's χ^2 (2, $n = 673$) = 172.8, $p < 0.0001$); 50% of standing trees had severe branch damage compared with 10% of saplings.

The storm surge deposited a layer of marine carbonate mud of varying thickness at most of the sites (Table 1, Fig. 2b). The fringe plot on Mud Key had a drastically different substrate than the other plots (substrate was eroding and composed of

Fig. 2 Example of a heavily damaged forest on Waltz Key in the Lower Florida Keys, 6 months post-storm (**a**), carbonate mud storm surge deposit (**b**), and *Avicennia germinans* epicormic growth at Fakahatchee Bay in the Ten Thousand Islands, 9 months post-storm (**c**)

an overwash berm of coral fragments and loose carbonate sand, with no visible peat or mud storm deposit) and thus was excluded from mud storm deposit analyses. The thickness of the carbonate mud storm deposit was examined to determine its impact on delayed mangrove mortality (defined here as an increase in percent tree mortality from November/December 2017 to June 2018). Although storm deposit depth had no significant influence on the initial mortality of the trees, it was significantly related to delayed tree mortality (Table 2, Fig. 6a). There were no significant differences in basal area, tree height, or proportion of trees with severe branch damage among the plots in the three storm deposit categories (ANOVA p values > 0.05). The saplings did not have a significant trend in delayed mortality with relation to storm deposit categories (Fig. 6b; Kruskal–Wallis χ^2 (2) = 5.5840, $p = 0.061$). Seedling density also did not vary significantly between the storm deposit categories during any monitoring effort (ANOVA p values > 0.05).

Average soil shear strength was 24.7 ± 10.2 kPa in the Lower Florida Keys and 16.9 ± 3.8 kPa in the Ten Thousand Islands. Region and soil depth had a significant effect on soil shear strength (Table 3, Fig. 7a), although forest type (fringe vs. basin) had no significant effect. Subterranean roots grew at an average rate of 0.16 g m^{-2} $month^{-1}$ in the Lower Florida Keys (range 0.01–0.45 g m^{-2} $month^{-1}$), and 4.37 g m^{-2} $month^{-1}$ in the Ten Thousand Islands (range 0.76–11.02 g m^{-2} $month^{-1}$). Root growth rates varied significantly by region, but not by forest type or by storm deposit depth (Table 3, Fig. 7b). There were no significant correlations between root growth rate and mangrove height (Pearson's correlation coefficient = 0.45, $p = 0.090$, $n = 15$), nor between root growth rate and abundance of the three mangrove species (Pearson's correlation p values > 0.05, $n = 14$).

Discussion

Trends in Initial Damage and Delayed Mortality

Larger trees are often more susceptible to damage than smaller trees during wind events (Roth 1992; Doyle et al. 1995; Imbert et al. 1996; Kovacs et al. 2001; Feller et al. 2015; Villamayor et al. 2016), although some studies have found that mangrove trees in the largest diameter classes have higher survival than moderately sized trees (Smith III et al. 1994; McCoy et al. 1996). This study found that trees with a D_{130} from 5 to 10 cm suffered less severe branch damage than larger trees, and saplings ($D_{130} < 5$ cm) had lower rates of mortality and severe branch damage than trees. The degree of extensive branch damage in trees likely contributed to

Table 1 Summary of 18 vegetation plots. Data are reported as average values for each plot, ±SD if applicable, as determined from monitoring data in June 2018 (9 months post-storm). Tree mortality is presumably attributable to the hurricane or its aftereffects (decaying trees are excluded)

	Location	Latitude and longitude	Forest type	Carbonate mud storm deposit[1]	Mangrove height (m)	Soil strength (kPa, 25 cm depth)	% tree mortality	Root growth rate[4] (g m^{-2} $month^{-1}$)	% canopy coverage
Lower Florida Keys	Upper Saddlebunch Key	24.65060 –81.59628	Basin	Minimal to none	1.5 ± 0.2	15.8 ± 13.2	N/A[3]	0.40 ± 0.50	24 ± 25
	Upper Saddlebunch Key	24.64996 –81.59640	Fringe	Minimal to none	3.7 ± 0.6	66.4 ± 10.8	13.3	0.01 ± 0.00	93 ± 7
	Lower Snipe Key	24.66221 –81.61012	Basin	Thick	8.5 ± 3.2	11.4 ± 7.7	54.8	0.04 ± 0.04	75 ± 8
	Lower Snipe Key	24.66247 –81.60942	Fringe	Moderate	6.4 ± 1.1	14.8 ± 8.3	26.9	0.32 ± 0.01	76 ± 16
	Mud Key	24.67688 –81.70148	Basin	Moderate	2.2 ± 0.3	26.4 ± 13.7	20.0	0.01 ± 0.01	48 ± 16
	Mud Key	24.67726 –81.70131	Fringe	N/A[2]	6.1 ± 0.9	41.2 ± 24.8	16.0	N/A	42 ± 24
	Middle Snipe Key	24.67851 –81.65391	Basin	Thick	7.8 ± 3.1	43.4 ± 7.3	56.5	N/A	81 ± 23
	Middle Snipe Key	24.67903 –81.65326	Fringe	Moderate	5.7 ± 1.0	20 ± 13.4	25.0	0.13 ± 0.01	44 ± 20
	Middle Snipe Key	24.67766 –81.65486	Fringe	Thick	5.8 ± 0.9	20.6 ± 13.9	100.0	0.03 ± 0.01	22 ± 12
	Waltz Key	24.64777 –81.65367	Fringe	Moderate	5.5 ± 1.4	17.2 ± 13.9	22.6	0.45 ± 0.60	90 ± 7
	Waltz Key	24.64764 –81.65342	Fringe	Thick	7.8 ± 1.2	15.8 ± 12.3	30.3	0.08 ± 0.07	42 ± 26
Ten Thousand Islands	Blackwater Bay	25.92503 –81.60809	Fringe	Thick	8.1 ± 2.0	11.2 ± 8.5	35.0	0.76 ± 0.87	32 ± 7
	Blackwater Bay	25.92356 –81.61274	Basin	Thick	5.4 ± 1.7	23.2 ± 7.2	10.5	3.14 ± 3.14	70 ± 17
	Cat's Claw Basin	26.02173 –81.73376	Basin	Minimal to none	8.6 ± 2.5	29.6 ± 9.3	6.1	11.0 ± 12.6	77 ± 10
	Fakahatchee Bay	25.88797 –81.50747	Fringe	Minimal to none	9.0 ± 2.1	27.4 ± 11.1	31.3	2.68 ± 3.43	48 ± 17
	Fakahatchee Bay	25.88798 –81.50507	Basin	Moderate	9.6 ± 1.1	28.0 ± 18.2	13.2	0.80 ± 0.30	62 ± 8
	Faka Union Canal	25.90194 –81.51102	Fringe	Minimal to none	10.6 ± 2.7	18.2 ± 5.6	22.7	N/A	73 ± 10
	Faka Union Canal	25.90186 –81.51057	Basin	Thick	9.9 ± 3.3	13.4 ± 7.1	19.6	7.84 ± 2.91	52 ± 13

[1] Minimal to none (0–0.2 cm), moderate (0.2–1 cm), or thick (1–9 cm)

[2] Overwash of coral and other carbonate fragments

[3] Scrub mangrove site, no trees ($D_{130} > 5$ cm) present in plot

[4] Root in-growth bags incubated for 4 months in the Lower Florida Keys and 6 months in Ten Thousand Islands. Not all plots included root in-growth bags

Table 2 Effects of region (Lower Florida Keys or Ten Thousand Islands), forest type (fringe or basin), and storm deposit category (minimal to none 0–0.2 cm, moderate 0.2–1 cm, or thick 1–9 cm) on initial tree mortality (proportion of trees initially killed 2–3 months post-storm) and delayed tree mortality (percent increase in mortality from 2 to 3 months post-storm to 9 months post-storm)

Effect	Initial tree mortality			Delayed tree mortality		
	df	*F*	*p*	df	*F*	*p*
Region	1,6	0.07	0.804	1,6	8.48	0.027
Forest type	1,6	0.53	0.495	1,6	0.01	0.929
Storm deposit	2,6	0.02	0.977	2,6	11.66	0.009
Region × forest type	1,6	0.25	0.637	1,6	8.73	0.026
Forest type × storm deposit	2,6	0.38	0.699	2,6	0.76	0.509
Region × storm deposit	2,6	2.06	0.209	2,6	1.56	0.285

delayed mortality (Fig. 5c). Bruising and damage to the vascular system, defoliation, and loss of branches can all cause stress and eventual mortality to trees months after a severe wind event (Craighead and Gilbert 1962; Shaw 1983; Everham and Brokaw 1996). Large trees can shield understory trees from the strongest winds and protect them from damage (Imbert et al. 1996; Zhang et al. 2008). Trees with smaller stem sizes (and smaller canopy) are also more likely to bend in the wind rather than break (Cremer et al. 1982; Doyle et al. 1995; Everham and Brokaw 1996; Swiadek 1997). The frequency of tropical cyclones has also been found to be one of the factors limiting mangrove growth and contributing to global trends in mangrove canopy height (Simard et al. 2019).

Although the degree of branch damage was greater in larger trees (Fig. 5b), this study did not find a significant trend in mortality across tree size classes (Fig. 5c). This may be attributable to the relatively small size of the mangrove forests in this study (Simard et al. 2019). Average mangrove height across the plots ranged from 1.5–10.6 m (Table 1), and the majority of trees within these plots had stem diameters < 10 cm (Fig. 5a). The two basin plots in our study (Upper Saddlebunch Key and Mud Key) that were dominated by scrub mangroves with average heights < 2.2 m had low mangrove mortality and low branch damage, similar to previous studies which have found that the low stature of scrub mangroves helps to protect the vegetation from wind exposure (Smith III et al. 1994; Doyle et al. 2009). Small mangroves near the shore may also have been partially submerged by storm surge and protected from wind damage during the hurricane (Smith III et al. 1994).

If large trees topple during a storm, they can cause indirect damage by falling on adjacent trees and crushing the understory. The direction of treefall can provide an indication of the wind direction and thus time during the hurricane when the majority of the damage occurred (Doyle et al. 1995, 2009; Everham and Brokaw 1996). Assessment of treefall direction was initially attempted in this study, but the severity of damage and occurrence of treefall due to secondary damage hindered accurate directional determination. It was also not possible to gauge the severity of damage with respect to distance from the hurricane eyewall (Smith III et al. 1994; Milbrandt et al. 2006) as nearly all sites were within the eyewall radius of Hurricane Irma.

Trees in this study also suffered delayed mortality as a result of the smothering of their root system by the carbonate mud storm deposit (Fig. 6a). Mortality of *Avicennia* spp. can occur when their pneumatophores are partially or entirely covered by sediment (Allingham and Neil 1996; Lee et al. 1996; Ellison 1998). While *Rhizophora* spp. have extensive aerial prop roots that extend high above the surface of the soil, the lenticels (respiratory pores) on these roots are clustered in highest densities near the soil surface (Gill and Tomlinson 1977). Thus, excess sedimentation, including storm surge deposition, can also cause mortality in the *Rhizophora* genus when these lenticels are buried (Terrados et al. 1997; Ellison 1998). The thickness of the storm deposit did not have a significant impact on delayed mortality in saplings (Fig. 6b). This may be the result of the growth of seedlings into saplings during the duration of the study, adding to the pool of saplings. Saplings also had less branch damage than trees and therefore did not have to cope with as many compounding stress factors. The impacted sites may continue to see delayed mortality for several years, as mortality in Florida mangroves has been found to increase for up to 3 years following a hurricane (Barr et al. 2012).

Soil Strength and Root Growth

Although Cahoon et al. (2003) noted significantly higher soil shear strength in fringe mangroves compared with basin forests, this study did not find any significant differences by forest type (Fig. 7a, Table 3). However, the four greatest shear strengths observed at any of the sites were at Lower Florida Keys fringe forests. The lack of a significant difference between fringe and basin forests may, in part, be due to the confounding influence of soft surficial storm deposits. These

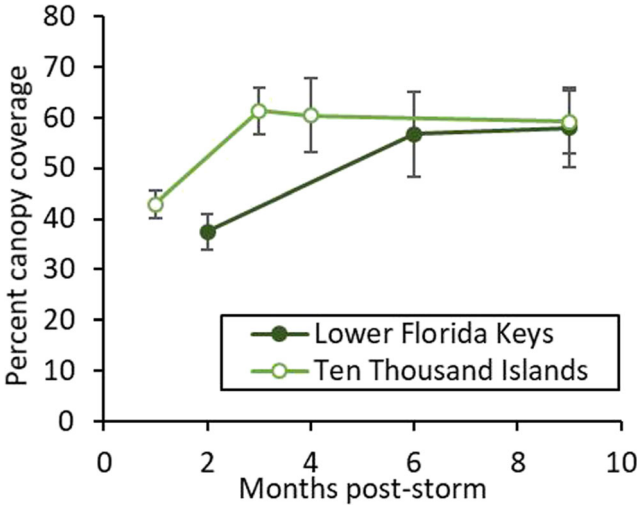

Fig. 3 Canopy coverage in the Lower Florida Keys and Ten Thousand Islands following Hurricane Irma. Values are means across all vegetation plots; error bars denote standard error of the mean (SEM)

surface values should not be considered representative of mangrove peat due to the presence of these soft storm deposits. Soil shear strength varied with depth (Table 3). Most sites had lower shear strength at 50-cm depth; this presumably reflects the contribution of root density to soil strength, as most mangrove roots are found in the top 30 cm of soil (Komiyama et al. 2000).

Root growth rates in this study varied from 0.01–11.0 g m^{-2} $month^{-1}$, with an average of 0.16 g m^{-2} $month^{-1}$ in the Lower Florida Keys and 4.37 g m^{-2} $month^{-1}$ in the Ten Thousand Islands. It should be noted that root growth into root bags may not necessarily reflect natural growth rates, because root growth may increase as roots propagate into the unoccupied soil in the root bags or may be slower as a result of disturbance from the coring process necessary for bag

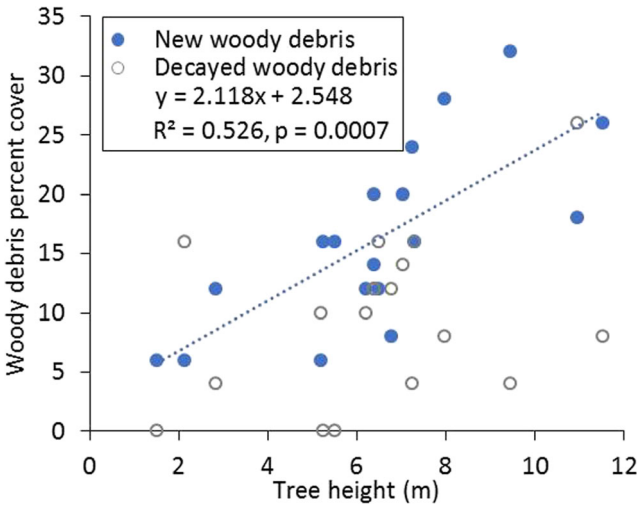

Fig. 4 Percent cover on the forest floor of newly felled and decayed woody debris as a function of tree height. Data are from November and December 2017 in the Lower Florida Keys and Ten Thousand Islands, respectively

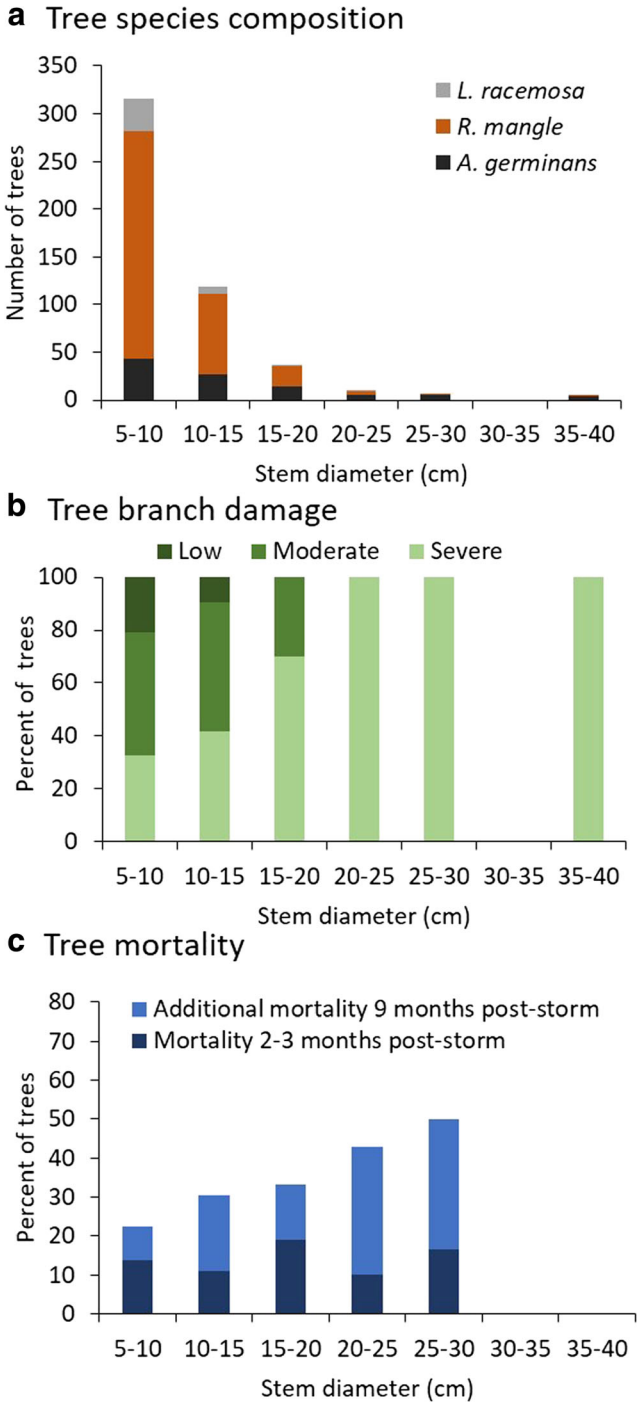

Fig. 5 Species composition of all mangrove trees (live and dead) by stem diameter (D_{130}) (**a**), live tree branch damage, as determined 2–3 months post-storm (**b**), and initial mortality and delayed mortality in the Lower Florida Keys and Ten Thousand Islands following Hurricane Irma (**c**)

insertion (Vogt et al. 1998; McKee and Faulkner 2000). This method does, however, allow for comparison among sites where similar root in-growth bag methods have been applied. The growth rates in this study are low compared with previous studies from Florida mangroves. McKee and Faulkner (2000) found that root production in the top 30 cm of soil in

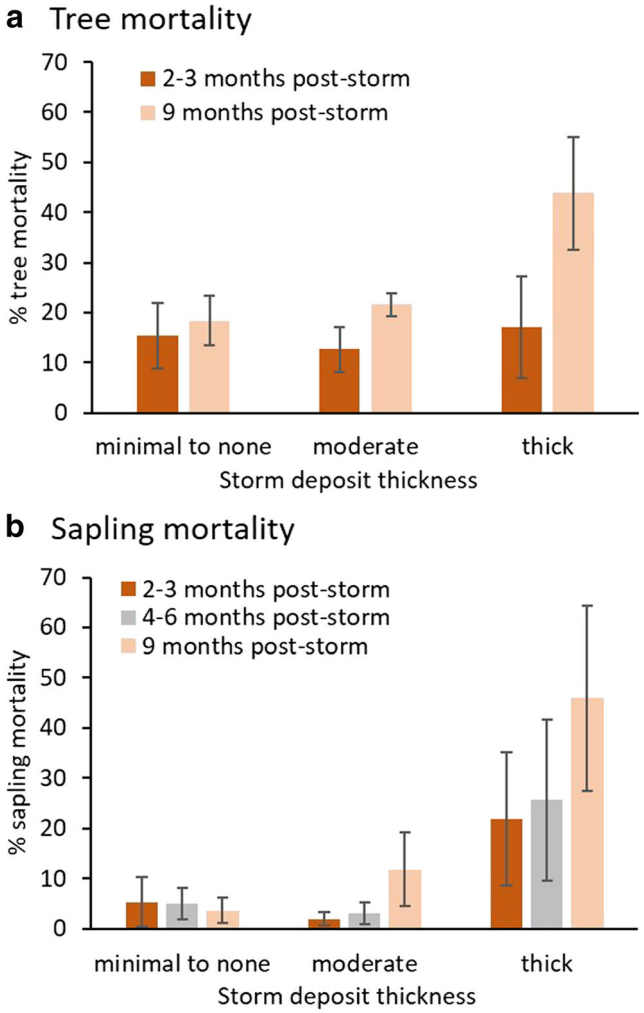

Fig. 6 Tree mortality (**a**) and sapling mortality (**b**) at plots with a differing thickness of storm deposits in the Lower Florida Keys and Ten Thousand Islands following Hurricane Irma. Carbonate mud storm deposit thickness classified as minimal to none (0–0.2 cm, $n = 4$ plots for trees, 5 for saplings), moderate (0.2–1 cm, $n = 5$ plots), or thick (1–9 cm, $n = 7$ plots). Error bars denote SEM

southwest Florida mangroves varied from 0.05–3.14 g m^{-2} d^{-1} (equivalent of 1.5–94.2 g m^{-2} $month^{-1}$). Sánchez (2005) used similar methods in the Ten Thousand Islands region and documented rates of root growth of 106–842 g m^{-2} $yr.^{-1}$ (8.8–70 g m^{-2} $month^{-1}$). Cahoon et al. (2003) found that root growth rates varied from 0 to 656 g m^{-2} yr^{-1} (0–54.6 g m^{-2} $month^{-1}$) in hurricane-impacted mangrove forests in Honduras; in that study, sites with the most severe hurricane impacts had no root growth. The low rates of root growth seen in this study were likely a consequence of both tree mortality and reduced oxygen exchange as a result of the surficial storm deposit. Root growth may be limited if roots do not have sufficient oxygen for respiration or if soil is excessively water-logged (Gregory 1987; Sorrell and Armstrong 1994). This study did not find a significant difference between root production at the fringe and basin forests, similar to the findings of Cahoon et al. (2003) on root growth in hurricane-impacted mangroves. Higher root growth rates in the Ten Thousand Islands compared with the Lower Florida Keys may partly be due to the longer incubation time (6 months vs. 4 months) as well as the fact that the incubation time in the Ten Thousand Islands included some warmer summer months when mangroves have the highest growth rate (Lugo and Snedaker 1974). It also may reflect lower mangrove mortality in the Ten Thousand Islands (20% vs. 36% mortality in the Lower Florida Keys).

Should trends in delayed mortality and low root growth continue, some of the mangrove forests in this study may be at risk of peat collapse. Mangrove peat is primarily produced through the accumulation of subterranean roots, with smaller contributions from the deposition of aboveground biomass (McKee and Faulkner 2000; Middleton and McKee 2001; Chmura et al. 2003). Vertical accumulation of peat depends upon the rate of peat production exceeding the rate of organic matter decomposition (Macintyre et al. 1995; Cahoon et al. 2003; McCloskey and Liu 2013). Mangrove forests with high tree mortality following a hurricane may face peat collapse as a result of compaction and continued decomposition of dead roots and organic matter without concurrent root growth (Cahoon et al. 2003; Barr et al. 2012). Barr et al. (2012) found that loss of elevation in a south Florida mangrove forest was strongly correlated with tree mortality following Hurricane Wilma; forest elevation declined by more than two centimeters over 3 years in sites with the highest rates of tree mortality. Peat collapse following hurricane-induced mortality has been hypothesized to be the cause of elevation loss and the conversion of mangrove forests to mud flats in southwest Florida (Wanless et al. 1995; Swiadek 1997; Smith III et al. 2009).

Early Signs of Recovery

After an initial increase from 40% canopy cover 1–2 months post-storm to 60% cover 3–6 months post-storm, canopy regrowth stagnated and canopy cover failed to increase in the following months (Fig. 3). For comparison, canopy coverage in an undisturbed south Florida mangrove forest is typically 90–95% (Milbrandt et al. 2006). The increase and plateau of canopy coverage in this study reflected initial regrowth (including epicormic growth, Fig. 2), but widespread branch damage and delayed tree mortality prevented more extensive growth 9 months post-storm.

Long-term recovery of the forest canopy will depend on regrowth of canopy branches as well as the "release" of established seedlings and saplings in the understory that grow rapidly in response to increased light levels below gaps in the canopy (Everham and Brokaw 1996; Sherman et al. 2001). Although they provide ample light, canopy gaps can also make survival more challenging for seedlings as they result in low-humidity and high-temperature conditions (Smith III

Table 3 Effects of region (Lower Florida Keys or Ten Thousand Islands), forest type (fringe or basin), soil depth (0, 25, and 50 cm), and monitoring round (2–3, 4–6, or 9 months post-storm) on soil shear strength. Effects of region, forest type, and storm deposit category (minimal to none 0–0.2 cm, moderate 0.2–1 cm, or thick 1–9 cm) on subterranean root growth rate

Soil shear strength				Root growth rate			
Effect	df	*F*	*p*	Effect	df	*F*	*p*
Region	1,147	6.35	0.013	Region	1,5	55.23	<0.001
Forest type	1,147	0.05	0.830	Forest type	1,5	0.37	0.567
Soil depth	2,147	4.85	0.009	Storm deposit	2,5	0.74	0.521
Monitoring round	2,147	1.22	0.300	Region × forest type	1,5	0.12	0.744
Region × forest type	1,147	0.76	0.383	Forest type × storm deposit	2,5	6.37	0.042
Region × soil depth	2,147	2.86	0.061	Region × storm deposit	2,5	0.09	0.912
Forest type × soil depth	2,147	0.24	0.785				

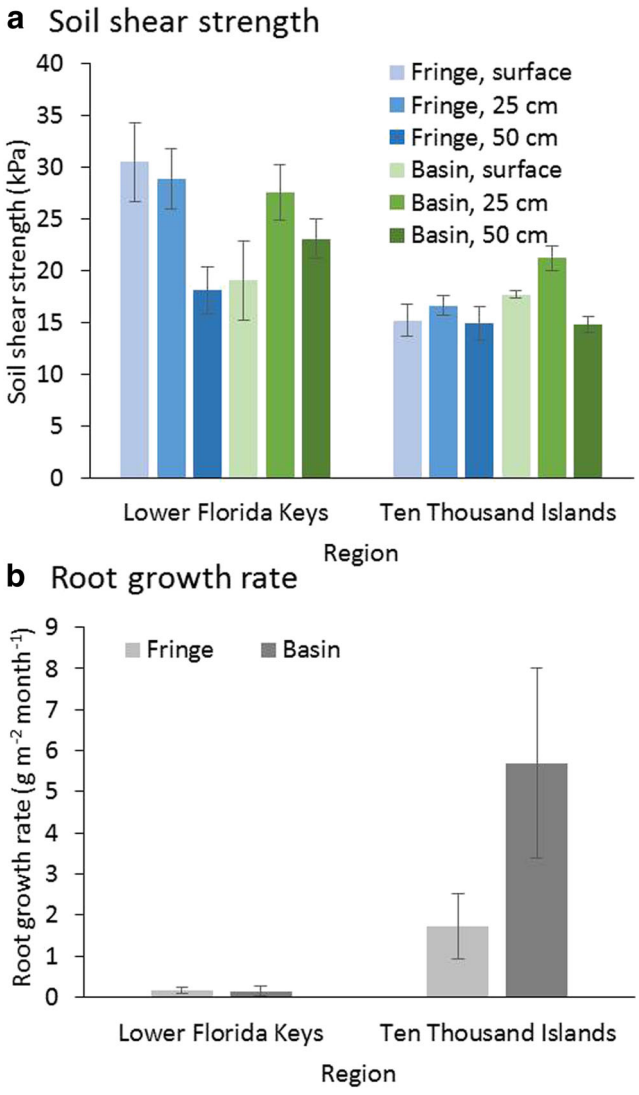

Fig. 7 Soil shear strength (grand mean of all measurements) (**a**) and subterranean root growth rates (**b**) in fringe and basin plots in the Lower Florida Keys and Ten Thousand Islands. Error bars denote SEM

et al. 1994; Swiadek 1997; Barr et al. 2012). If mortality is extensive and there are no longer live mangrove roots to aerate the soil, this can result in decreased redox potential and increased sulfide concentration, which may slow recolonization by seedlings (Smith III et al. 1994; Swiadek 1997).

The species composition of a forest following a disturbance event will largely depend upon the species composition of the understory (Everham and Brokaw 1996). The recovery of mangrove forests is also impacted by the density and species composition of available propagules, which largely depend on forest fragmentation and degree of hydrologic connectivity with live mangrove forests (Milbrandt et al. 2006). The relative abundance of the three dominant mangrove species may shift during the recovery process as a result of variable understory composition and propagule availability (Craighead 1971; Smith III et al. 1994; Imbert et al. 1996; Baldwin et al. 2001). In this study, *R. mangle* dominated the exposed understory and comprised 90% of all seedlings. By comparison, 79% of saplings and 75% of all live trees were *R. mangle*. *L. racemosa* seedlings require high amounts of light and thus are generally not found in great abundance in the mangrove understory (Wadsworth and Englerth 1959; Ball 1980). *A. germinans* and *L. racemosa* propagules mature in the late summer and early fall (Rabinowitz 1978; Tomlinson 1994). The occurrence of a hurricane in mid-September stripped away both leaves and propagules from the mangrove canopy and the storm surge presumably washed away unattached propagules. The lack of *A. germinans* and *L. racemosa* propagules was noted during field efforts, but not directly quantified. It is possible that hurricanes, including Irma, may contribute to a shift in species composition toward *R. mangle* due to their dominance in the understory and removal of propagules of other mangrove species (Swiadek 1997; Piou et al. 2006). Species shifts toward *Rhizophora* have also been noted as a result of variable species tolerances of sediment deposits. Lee et al. (1996) found that *Rhizophora* spp. overtook a

mangrove forest of *Avicennia* spp. after sediment deposits smothered pneumatophores. However, other studies have found *L. racemosa* experienced lower mortality than other mangrove species following a hurricane (Sherman et al. 2001). Long-term monitoring of the recovery process is needed to determine if species composition will truly shift or if thinning of the *R. mangle* understory, regrowth of established *L. racemosa* and *A. germinans* trees, and subsequent propagule dispersal during future years will be sufficient to maintain current species diversity.

In conclusion, this study has demonstrated that significant delayed tree mortality can occur months after a hurricane has passed. Further mortality may continue to occur as a result of ongoing root smothering by storm deposits and stress due to loss of canopy. Yet, signs of recovery were evident in the proliferation of *R. mangle* seedlings and partial regrowth of the forest canopy. Forest recovery trajectories will depend on regrowth of the surviving canopy, development of the existing understory, and recruitment and survival of new propagules. Not all sites may recover into a similar mangrove forest, and locations with high tree mortality and limited root growth are at risk of peat collapse if mortality trends persist. Continued monitoring is necessary to determine the full impacts of this hurricane and the resulting species composition of the recovering forest.

Acknowledgments Field assistance and laboratory support were provided by B Halavik, J Jacobs, B Rosenheim, C Schafer, JM Smoak, S Snader, J Walker, and E Wennick. Site access and research permission were provided by B Jessen for the Rookery Bay National Estuarine Research Reserve, M Danaher for the Ten Thousand Islands National Wildlife Refuge (Special Use Permit 41555-2017-R2), and K Watts for the Florida Keys National Wildlife Refuges Complex (Special Use Permit #FFO4RFKD-2015-020). We are grateful for assistance with study design and logistical support provided by SE Engelhart, BP Horton, and AC Kemp, as well as the helpful reviews and comments provided by the Estuaries and Coasts special issue editors and two anonymous reviewers. N.S.K. is supported by Singapore Ministry of Education Academic Research Fund Tier 2 MOE 2018-T2-1-030.

Funding Information Funding was provided through grants to RP Moyer by the National Fish & Wildlife Foundation (Grant ID: 2320.17.059025) and BP Horton by the National Science Foundation (OCE-1458903) and in-kind services by the US Geological Survey St. Petersburg Coastal and Marine Science Center.

References

Allingham, D.P., and D.T. Neil. 1996. The supratidal deposits and effects of coral dredging on Mud Island, Moreton Bay, Southeast Queensland. *Oceanographic Literature Review* 4 (43): 411.

Baldwin, A.H., W.J. Platt, K.L. Gathen, J.M. Lessmann, and T.J. Rauch. 1995. Hurricane damage and regeneration in fringe mangrove forests of Southeast Florida, USA. *Journal of Coastal Research* SI (21): 169–183.

Baldwin, A., M. Egnotovich, M. Ford, and W. Platt. 2001. Regeneration in fringe mangrove forests damaged by hurricane Andrew. *Plant Ecology* 157 (2): 151–164.

Ball, M.C. 1980. Patterns of secondary succession in a mangrove forest of southern Florida. *Oecologia* 44 (2): 226–235.

Barr, J.G., V. Engel, T.J. Smith, and J.D. Fuentes. 2012. Hurricane disturbance and recovery of energy balance, CO_2 fluxes and canopy structure in a mangrove forest of the Florida Everglades. *Agricultural and Forest Meteorology* 153: 54–66.

Breithaupt, J.L., J.M. Smoak, V.H. Rivera-Monroy, E. Castañeda-Moya, R.P. Moyer, M. Simard, and C.J. Sanders. 2017. Partitioning the relative contributions of organic matter and mineral sediment to accretion rates in carbonate platform mangrove soils. *Marine Geology* 390: 170–180.

Cahoon, D.R., P. Hensel, J. Rybczyk, K.L. McKee, C.E. Proffitt, and B.C. Perez. 2003. Mass tree mortality leads to mangrove peat collapse at Bay Islands, Honduras after Hurricane Mitch. *Journal of Ecology* 91 (6): 1093–1105.

Cangialosi, J.P., A.S. Latto, and R. Berg. 2018. National Hurricane Center Tropical Cyclone Report. Hurricane Irma (AL 112017) 30 August – 12 September 2017. National Hurricane Center. https://www.nhc.noaa.gov/data/tcr/AL112017_Irma.pdf. Accessed 15 March 2019

Castañeda-Moya, E., R.R. Twilley, V.H. Rivera-Monroy, K. Zhang, S.E. Davis, and M. Ross. 2010. Sediment and nutrient deposition associated with Hurricane Wilma in mangroves of the Florida Coastal Everglades. *Estuaries and Coasts* 33 (1): 45–58.

Chmura, G.L., S.C. Anisfeld, D.R. Cahoon, and J.C. Lynch. 2003. Global carbon sequestration in tidal, saline wetland soils. *Global Biogeochemical Cycles* 17 (4): 22 1–12. https://doi.org/10.1029/2002GB001917.

Craighead, F.C. 1971. *The trees of south florida*. Vol. Vol. 1. Coral Gables, FL: University of Miami Press.

Craighead, F.C., and V.C. Gilbert. 1962. The effects of Hurricane Donna on the vegetation of southern Florida. *Quarterly Journal of the Florida Academy of Sciences* 25 (1): 1–28.

Cremer, K.W., C.J. Borough, F.H. McKinnell, and P.R. Carter. 1982. Effects of stocking and thinning on wind damage in plantations. *New Zealand Journal of Forestry Science* 12 (2): 244–268.

Doyle, T.W., T.J. Smith III, and M.B. Robblee. 1995. Wind damage effects of Hurricane Andrew on mangrove communities along the southwest coast of Florida, USA. *Journal of Coastal Research* SI (21): 159–168.

Doyle, T.W., K.W. Krauss, and C.J. Wells. 2009. Landscape analysis and pattern of hurricane impact and circulation on mangrove forests of the Everglades. *Wetlands* 29 (1): 44–53.

Ellison, J.C. 1998. Impacts of sediment burial on mangroves. *Marine Pollution Bulletin* 37 (8–12): 420–426.

Everham, E.M., and N.V. Brokaw. 1996. Forest damage and recovery from catastrophic wind. *The Botanical Review* 62 (2): 113–185.

Feller, I.C., E.M. Dangremond, D.J. Devlin, C.E. Lovelock, C.E. Proffitt, and W. Rodriguez. 2015. Nutrient enrichment intensifies hurricane impact in scrub mangrove ecosystems in the Indian River Lagoon, Florida, USA. *Ecology* 96 (11): 2960–2972.

FNAI and FWC 2016. Cooperative land cover map. Florida Natural Areas Inventory and Florida Fish and Wildlife Conservation Commission. http://www.fnai.org/landcover.cfm . Accessed 15 March 2019.

Gill, A.M., and P.B. Tomlinson. 1977. Studies on the growth of red mangrove (*Rhizophora mangle* L.) 4. The adult root system. *Biotropica* 9 (3): 145–155.

Gregory, P.J. 1987. Development and growth of root systems in plant communities. In *Root development and function*, ed. P.J. Gregory and D.A. Rose, 147–166. Cambridge: Cambridge University Press.

Han, X., L. Feng, C. Hu, and P. Kramer. 2018. Hurricane-induced changes in the Everglades National Park mangrove forest: Landsat observations between 1985 and 2017. *Journal of Geophysical Research: Biogeosciences* 123 (11): 3470–3488. https://doi.org/10.1029/2018JG004501.

Imbert, D. 2018. Hurricane disturbance and forest dynamics in east Caribbean mangroves. *Ecosphere* 9 (7): e02231. https://doi.org/10.1002/ecs2.2231.

Imbert, D., P. Labbe, and A. Rousteau. 1996. Hurricane damage and forest structure in Guadeloupe, French West Indies. *Journal of Tropical Ecology* 12 (5): 663–680.

Komiyama, A., S. Havanond, W. Srisawatt, Y. Mochida, K. Fujimoto, T. Ohnishi, S. Ishihara, and T. Miyagi. 2000. Top/root biomass ratio of a secondary mangrove (*Ceriops tagal* (Perr.) CB Rob.) forest. *Forest Ecology and Management* 139 (1–3): 127–134.

Kovacs, J.M., M. Blanco-Correa, and F. Flores-Verdugo. 2001. A logistic regression model of hurricane impacts in a mangrove forest of the Mexican Pacific. *Journal of Coastal Research* 17 (1): 30–37.

Krauss, K.W., K.L. McKee, C.E. Lovelock, D.R. Cahoon, N. Saintilan, R. Reef, and L. Chen. 2014. How mangrove forests adjust to rising sea level. *New Phytologist* 202 (1): 19–34.

Lee, S.K., W.H. Tan, and S. Havanond. 1996. Regeneration and colonisation of mangrove on clay-filled reclaimed land in Singapore. *Hydrobiologia* 319 (1): 23–35.

Lewis, R.R., III, E.C. Milbrandt, B. Brown, K.W. Krauss, A.S. Rovai, J.W. Beever III, and L.L. Flynn. 2016. Stress in mangrove forests: Early detection and preemptive rehabilitation are essential for future successful worldwide mangrove forest management. *Marine Pollution Bulletin* 109 (2): 764–771.

Lugo, A.E., and S.C. Snedaker. 1974. The ecology of mangroves. *Annual Review of Ecology and Systematics* 5 (1): 39–64.

Macintyre, I.G., M.M. Littler, and D.S. Littler. 1995. Holocene history of Tobacco Range, Belize, Central America. *Atoll Research Bulletin* 430: 1–18.

McCloskey, T.A., and K.B. Liu. 2013. Sedimentary history of mangrove cays in Turneffe Islands, Belize: Evidence for sudden environmental reversals. *Journal of Coastal Research* 29 (4): 971–983.

McCoy, E.D., H.R. Mushinsky, D. Johnson, and W.E. Meshaka Jr. 1996. Mangrove damage caused by Hurricane Andrew on the southwestern coast of Florida. *Bulletin of Marine Science* 59 (1): 1–8.

McKee, K.L. 2001. Root proliferation in decaying roots and old root channels: A nutrient conservation mechanism in oligotrophic mangrove forests? *Journal of Ecology* 89 (5): 876–887.

McKee, K.L., and P.L. Faulkner. 2000. Restoration of biogeochemical function in mangrove forests. *Restoration Ecology* 8 (3): 247–259.

Middleton, B.A., and K.L. McKee. 2001. Degradation of mangrove tissues and implications for peat formation in Belizean island forests. *Journal of Ecology* 89 (5): 818–828.

Milbrandt, E.C., J.M. Greenawalt-Boswell, P.D. Sokoloff, and S.A. Bortone. 2006. Impact and response of Southwest Florida mangroves to the 2004 hurricane season. *Estuaries and Coasts* 29 (6): 979–984.

NOAA 2017. National Hurricane Center GIS Archive - Tropical Cyclone Best Track for AL112017. National Oceanic and Atmospheric Administration. https://www.nhc.noaa.gov/gis/archive_besttrack_results.php?id=al11&year=2017&name=Hurricane. Accessed 15 March 2019.

NOAA. 2019. Historical hurricane tracks. National Oceanic and Atmospheric Administration. https://coast.noaa.gov/hurricanes/ . Accessed 8 March 2019.

NWS. 2017a. *Hurricane Irma Forecast/Advisory 44*. Miami, FL: National Weather Service National Hurricane Center https://www.nhc.noaa.gov/archive/2017/al11/al112017.fstadv.044.shtml ? Accessed 15 March 2019.

NWS. 2017b. *Hurricane Irma Forecast/Advisory 45. National Weather Service National Hurricane Center*. FL: Miami https://www.nhc.noaa.gov/archive/2017/al11/al112017.fstadv.045.shtml ? Accessed 15 March 2019.

Piou, C., I.C. Feller, U. Berger, and F. Chi. 2006. Zonation patterns of Belizean offshore mangrove forests 41 years after a catastrophic hurricane. *Biotropica: The Journal of Biology and Conservation* 38 (3): 365–374.

Poulos, S.J. 1981. The steady state of deformation. *Journal of Geotechnical and Geoenvironmental Engineering* 107 (ASCE 16241 Proceeding).

Rabinowitz, D. 1978. Dispersal properties of mangrove propagules. *Biotropica* 10 (1): 47–57.

Risi, J.A., H.R. Wanless, L.P. Tedesco, and S. Gelsanliter. 1995. Catastrophic sedimentation from Hurricane Andrew along the southwest Florida coast. *Journal of Coastal Research* SI (21): 83–102.

Ross, M.S., J.J. O'Brien, and L.J. Flynn. 1992. Ecological site classification of Florida Keys terrestrial habitats. *Biotropica* 24 (4): 488–502.

Ross, M.S., P.L. Ruiz, J.P. Sah, D.L. Reed, J. Walters, and J.F. Meeder. 2006. Early post-hurricane stand development in fringe mangrove forests of contrasting productivity. *Plant Ecology* 185: 283–297.

Roth, L.C. 1992. Hurricanes and mangrove regeneration: Effects of Hurricane Joan, October 1988, on the vegetation of Isla del Venado, Bluefields, Nicaragua. *Biotropica* 24 (3): 375–384.

Sánchez, B.G. 2005. Belowground productivity of mangrove forests in southwest Florida. PhD Dissertation, Louisiana State University. https://digitalcommons.lsu.edu/gradschool_dissertations/1652.

Shaw, W.B. 1983. Tropical cyclones: Determinants of pattern and structure in New Zealand's indigenous forests. *Pacific Science* 37: 405–414.

Sherman, R.E., T.J. Fahey, and P. Martinez. 2001. Hurricane impacts on a mangrove forest in the Dominican Republic: Damage patterns and early recovery. *Biotropica* 33 (3): 393–408.

Shier, D.E. 1969. Vermetid reefs and coastal development in the Ten Thousand Islands, southwest Florida. *Geological Society of America Bulletin* 80 (3): 485–508.

Simard, M., L. Fatoyinbo, C. Smetanka, V.H. Rivera-Monroy, E. Castañeda-Moya, N. Thomas, and T. Van der Stocken. 2019. Mangrove canopy height globally related to precipitation, temperature and cyclone frequency. *Nature Geoscience* 12: 40–45. https://doi.org/10.1038/s41561-018-0279-1.

Sippo, J.Z., C.E. Lovelock, I.R. Santos, C.J. Sanders, and D.T. Maher. 2018. Mangrove mortality in a changing climate: An overview. *Estuarine, Coastal and Shelf Science* 215: 241–249. https://doi.org/10.1016/j.ecss.2018.10.011.

Smith, T.J., III, M.B. Robblee, H.R. Wanless, and T.W. Doyle. 1994. Mangroves, hurricanes, and lightning strikes. *BioScience* 44 (4): 256–262.

Smith, T.J., III, G.H. Anderson, K. Balentine, G. Tiling, G.A. Ward, and K.R. Whelan. 2009. Cumulative impacts of hurricanes on Florida mangrove ecosystems: Sediment deposition, storm surges and vegetation. *Wetlands* 29 (1): 24–34.

Sorrell, B.K., and W. Armstrong. 1994. On the difficulties of measuring oxygen release by root systems of wetland plants. *Journal of Ecology* 82 (1): 177–183.

Swiadek, J.W. 1997. The impacts of Hurricane Andrew on mangrove coasts in southern Florida: A review. *Journal of Coastal Research* 13 (1): 242–245.

Symbula, M., and F.P. Day Jr. 1988. Evaluation of two methods for estimating belowground production in a freshwater swamp forest. *American Midland Naturalist* 120 (2): 405–415.

Terrados, J., U. Thampanya, N. Srichai, P. Kheowvongsri, O. Geertz-Hansen, S. Boromthanarath, N. Panapitukkul, and C.M. Duarte. 1997. The effect of increased sediment accretion on the survival and growth of *Rhizophora apiculate* seedlings. *Estuarine, Coastal and Shelf Science* 45 (5): 697–701.

Tomlinson, P.B. 1980. *The biology of trees native to tropical Florida*. Allston, Massachusetts: Harvard University Printing Office.

Tomlinson, P.B. 1994. *The botany of mangroves*. Cambridge: University of Cambridge Press.

Villamayor, B.M.R., R.N. Rollon, M.S. Samson, G.M.G. Albano, and J.H. Primavera. 2016. Impact of *Haiyan* on Phillipine mangroves: Implications to the fate of the widespread monospecific *Rhizophora* plantations against strong typhoons. *Ocean & Coastal Management* 132: 1–14. https://doi.org/10.1016/j.ocecoaman.2016.07.011.

Vogt, K.A., D.J. Vogt, and J. Bloomfield. 1998. Analysis of some direct and indirect methods for estimating root biomass and production of forests at an ecosystem level. *Plant and Soil* 200: 71–89.

Wadsworth, F.H., and G.H. Englerth. 1959. Effects of the 1956 hurricane on forests in Puerto Rico. *Caribbean Forester* 20: 38–51.

Walker, L.R., D.J. Lodge, and R.B. Waide. 1991. An introduction to hurricanes in the Caribbean. *Biotropica* 23 (4): 313–316.

Wanless, H.R., L.P. Tedesco, J.A. Risi, B.G. Bischof, and S. Gelsanliter. 1995. The role of storm processes on the growth and evolution of coastal and shallow marine sedimentary environments in South Florida. Pre-Congress Field Trip Guidebook. The 1st SEPM Congress on Sedimentary Geology, August 13–16, 1995, St. Pete Beach, Florida, USA. Society for Sedimentary Geology, St. Petersburg, Florida, USA.

Willoughby, H.E., and M.E. Rahn. 2004. Parametric representation of the primary hurricane vortex. Part I: Observations and evaluation of the Holland (1980) model. *Monthly Weather Review* 132 (12): 3033–3048.

Zhang, K., M. Simard, M. Ross, V.H. Rivera-Monroy, P. Houle, P. Ruiz, R.R. Twilley, and K. Whelan. 2008. Airborne laser scanning quantification of disturbances from hurricanes and lightning strikes to mangrove forests in Everglades National Park, USA. *Sensors* 8 (4): 2262–2292.